CrystEngComm

HIGHLIGHT

View Article Online
View Journal | View Issue

Cite this: *CrystEngComm*, 2024, **26**, 3771

Cobalt(II) coordination polymers with single-ion magnet property

Yi Wan, Yang-Lu Zhang, Qian Zhang, Shun-Yi Yang and Dong Shao *

Received 21st May 2024,
Accepted 25th June 2024

DOI: 10.1039/d4ce00512k

rsc.li/crystengcomm

Single-ion magnets (SIMs) are composed of 3d and/or 4f complexes with substantial energy barriers that inhibit spin reversal at the molecular level. The magnetic bistability of SIMs renders them promising for applications in quantum computing, high-density information storage, and molecular spintronics. Cobalt(II) ions are particularly advantageous among transition metals due to their high magnetic anisotropy, stability, and diverse coordination geometries. By integrating coordination frameworks with SIMs, a robust foundation has been established for the design and construction of novel molecular nanomagnets. This article provides an overview of single-ion magnetism within cobalt(II)-based coordination polymers, encompassing self-assemblies in one, two, and three dimensions. These findings underscore the potential of cobalt(II)-based coordination frameworks as a compelling platform for advancing the field of SIMs.

Introduction

Single-molecule magnets (SMMs) are molecular solids that exhibit a slow relaxation of their magnetization solely due to molecular properties.[1,2] They are of great interest for fundamental research into quantum effects and have potential applications in molecular spintronics and data storage.[3–5] Since the discovery of the first Mn_{12} SMM in 1993,[1] this field has rapidly expanded.[6–13] Significant advancements have been made in enhancing the magnetization reversal barriers (U_{eff}) and magnetic blocking temperatures (T_B), crucial parameters for evaluating the efficacy of a SMM. The barrier in transition-metal-based SMMs is characterized by $U = S^2|D|$ for integer spins or $U = (S^2 - 1/4)|D|$ for half-integer spins, where S represents the ground state spin and D is the axial zero-field splitting (ZFS) parameter. Initially, research focused on increasing the S of transition-metal clusters, but the barrier values remained low.[14] In 2010, Long *et al.* observed slow relaxation of the magnetization in a high-spin mononuclear Fe(II) complex, K[(tpa^{Mes})Fe], for the first time.[15] In 2011, the organometallic mononuclear Er(III) complex, (Cp*)Er(COT), was magnetically characterized by Gao and co-workers, sparking a notable expansion in the study of organometallic Ln-SIMs.[16] Subsequently, there has been a significant shift towards designing and constructing mononuclear SMMs, termed as single-ion magnets (SIMs), as they are liable to design and synthesize compared to their polynuclear counterparts, while also exhibiting larger magnetic anisotropy.[17–20] Over the past decade, a variety of 3d SIMs, including Cr^{2+}, $Fe^{1+/2+/3+}$, $Co^{1+/2+}$, $Ni^{1+/2+}$, Mn^{3+}, Cu^{2+}, and $Re^{3+/4+}$ ions, have been reported,[21–50] with Co(II) SIMs being particularly common and prominent in this group due to high air stability and significant magnetic anisotropy resulting from both orbital and spin contributions to the magnetic moment.[51] To date, numerous two- to eight-coordinated Co(II) SIMs with diverse structures, including linear, tetrahedral, square antiprism, pyramidal, square pyramidal, trigonal prismatic, octahedral, pentagonal bipyramidal geometries, have been successfully synthesized and characterized.[52–65] However, it remains a major synthetic challenge to incorporate specific coordination geometries into coordination polymers achieving remarkable magnetic anisotropy toward high-performance SIMs.

Magnetic anisotropy, which comes from both the Zeeman effect and zero field splitting, reflects how the magnetization of a transition metal complex will tend to orient preferentially along one or several directions.[9] The SIM performance is determined in part by large magnetic anisotropy. Generally, the following spin-Hamiltonian formalism is used to estimate the magnitude of ZFS parameters based on magnetic susceptibility and magnetization:

$$\hat{H} = D\left[\hat{s}_z - \frac{\hat{S}\left(\hat{S}+1\right)}{3}\right] + E\left(\hat{S}_x^2 - \hat{S}_y^2\right) + \mu_B g\cdot\hat{S}\cdot B \qquad (1)$$

where D and E are the axial and transverse ZFS, respectively, and $\hat{S}$ the spin operator.[18] The experimental determination of ZFS parameters is a complex process. Various techniques can be utilized to obtain these parameters, including indirect methods like magnetometry and magnetic circular dichroism (MCD), as well as direct methods such as inelastic neutron

Hubei Key Laboratory of Processing and Application of Catalytic Materials, College of Chemistry and Chemical Engineering, Huanggang Normal University, Huanggang 438000, P. R. China. E-mail: shaodong@nju.edu.cn

scattering (INS) and frequency domain magnetic resonance spectroscopy. High-frequency and high-field electronic paramagnetic resonance (HF-EPR) spectroscopy is the most widely used and powerful technique for determining ZFS parameters across a wide range of values. Additionally, significant theoretical advancements have led to the development of quantum chemical methodologies (CASSCF/NEVPT2/RASSI-SO/SINGLE_ANISO) for predicting ZFS parameters, providing insights into the magnetic anisotropy's physical origins and aiding in the interpretation of experimental data. Except the magnetic anisotropy, relaxation dynamics paly also a key effect on the magnetic performance of SIMs. The relaxation of magnetization in SIMs occurs through various mechanisms, such as the QTM, direct, Raman, and Orbach relaxation processes.[32] These processes can be described by the following equation including the sum of all four terms:

$$\tau^{-1} = {\tau_{\mathrm{QTM}}}^{-1} + AT + CT^{n} + {\tau_0}^{-1}\exp(-U_{\mathrm{eff}}/k_{\mathrm{B}}T) \quad (2)$$

where the first two terms are QTM and direct relaxation mechanisms. The three and four terms are field dependent Raman and field independent Orbach mechanisms. The relaxation mechanisms of SIMs are highly sensitive to numerous factors, such as heat, magnetic field, intermolecular interactions, and hyperfine interactions.[15] Thus, magnetic anisotropy and relaxation dynamics are two core research topics in the field of SIMs.

In recent years, the integration of SMMs with metal–organic frameworks (MOFs) has produced compelling outcomes in the realm of SMM-MOFs, providing new platform for the modulation of magnetic anisotropy and relaxation dynamics.[66–68] MOFs, characterized as crystalline porous structures consisting of metal ions or clusters interconnected by organic ligands, have garnered significant attention across diverse scientific domains.[69] In 2015, Shi and collaborators successfully synthesized a novel didysprosium MOF, where the Dy_2 dimers serve as serving as secondary building units (SBUs).[70] Noteworthy is the observation that this Dy_2-MOF undergoes guest exchange *via* crystal-to-crystal transformations, resulting in a reversible alteration of SMM properties. This finding underscores the potential of MOFs as a promising platform for modulating SMM behaviors. Recently, there also has been a growing interest in the construction of Co(II) coordination polymers that contain mononuclear Co^{2+} ions and exhibit slow relaxation of magnetization.[71–110] This trend represents a significant direction in the development of molecular framework nanomagnets. Theoretically, the spin dynamics of isolated magnetic molecules can be significantly enhanced by molecular vibrations.[110–112] By assembling Co(II) SIMs into rigid chains or frameworks, it is possible to tune the magnetic relaxation processes and metal–ligand vibrational modes. Furthermore, the properties of SIMs, such as relaxation dynamics and magnetic anisotropy, can be modified or controlled through crystal engineering design, leveraging the structural characteristics of coordination polymers. Currently, most complexes are constructed using distorted octahedral metal centers instead of the more distinct, highly anisotropic low-coordinate ones, resulting in relative worse SIM property. This preference is primarily due to the difficulty in synthesizing and maintaining the specific geometries chosen within a structure. Thus, the design and construction of Co(II) SIM coordination polymers need more endeavour and innovation. This review will discuss the advancements made in cobalt(II)-based coordination polymers exhibiting SIM property over the past decade, categorized by dimensionalities ranging from 1D to 2D and 3D, hoping to inspire more advances in this interesting direction (Fig. 1). It's worth noting that several outstanding reviews have been previously published focusing on the specific properties and chemistries of SIMs. For readers desiring more detailed references, we strongly recommend these reviews (ref. 6–10 and 17–20) to facilitate a deeper comprehension.

1D cobalt(II) SIMs

The design and preparation of 1D coordination compounds with specific topological structures, like zigzag, linear, spiral, and helical arrangements, poses a persistent synthetic challenge despite the simplicity of the 1D coordination array.[113] Linear and zigzag structures predominantly characterize these chains, with most of the previously reported 1D Co(II) SIMs being synthesized serendipitously. In 2015, Gao and co-workers reported a 1D cobalt(II) coordination polymer, $[Co(btm)_2(SCN)_2{\cdot}H_2O]_n$ (Fig. 2a),[71] that exhibited field-induced slow relaxation behavior with positive magnetic anisotropy. This study illustrates that a coordination polymer incorporating a SIM unit exhibits notable slow relaxation properties, offering a novel strategy for developing and synthesizing stable molecular magnetic materials using mononuclear complex units. This advancement contributes to the creation of multifunctional coordination polymer materials. Then, a number of 1D Co(II) compounds exhibiting SIM property were reported using distinct organic linkers and showing varying topologies (Table 1).[72–83] Notably, Wang and co-workers reported the structural and magnetic tuning in three homospin 1D chains constructed by a pentagonal bipyramidal Co^{II} building units and organic ligands of different lengths (Fig. 2b). Linear chain structures were observed in compounds with symmetric ligands, while a zigzag chain structure was found in the complex with an asymmetric linker. These findings highlight the use of a SIM building block approach in constructing Co(II) coordination chains. The magnetic interaction in these 1D chains plays a crucial role in slow magnetic relaxation. Furthermore, a novel cyano-bridged coordination nanotube was synthesized using pentagonal bipyramidal Co(II) building blocks and diamagnetic $[Co(CN)_6]^-$ anions. This nanotube exhibits field-induced slow magnetic relaxation, a behavior observed for the first time in coordination nanotubes (Fig. 2c).

It's well known that the predominant 1D coordination polymers exhibit both linear and zigzag structures. Nevertheless, the selective preparation of these two relatively straightforward chains remains challenging. In a recent study by

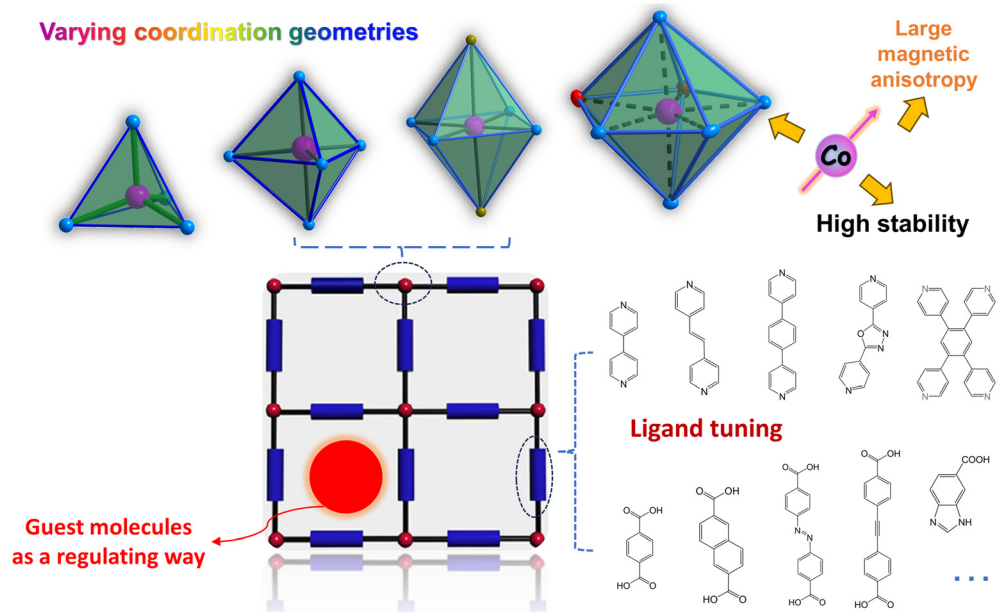

Fig. 1 Schematic illustration of cobalt(II)-based SIM coordination polymers.

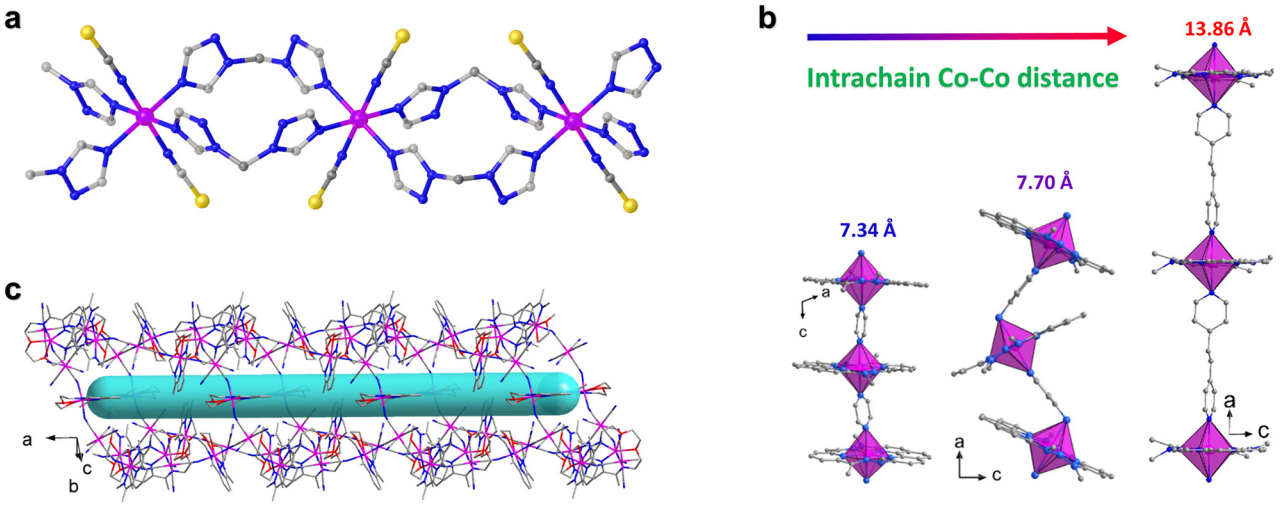

Fig. 2 (a) Structure of $[Co(btm)_2(SCN)_2{\cdot}H_2O]_n$;[71] (b) structures of three 1D chains constructed by a pentagonal bipyramidal Co^{II} building units and organic ligands of different lengths.[72] This figure has been reproduced from ref. 72 with permission from Royal Society of Chemistry, copyright 2016. (c) Structure of a cyano-bridged coordination nanotube.[73] This figure has been reproduced from ref. 73 with permission from Royal Society of Chemistry, copyright 2017.

Shao *et al.*, the terpyridine derivative was successfully combined with two distinct dicarboxylates to produce two novel 1D cobalt(II) coordination polymers.[81] This synthesis led to modifications in both the chain topological structures, easy-axis anisotropy, and relaxation dynamics, influenced by the unique bridging ligands of the dicarboxylic acids. The aforementioned findings not only showcase a route for fabricating 1D cobalt(II) coordination polymers with SIM characteristics but also present an opportunity to regulate chain configurations and magnetic anisotropy in 1D coordination polymers by employing diverse dicarboxylates.

Low-coordinate metallic ions are known for their ability to create high-performance single ion magnets due to their increased magnetic anisotropy. However, integrating these specific ions into coordination polymers remains a challenge. Currently, most complexes, including discrete polynuclear ones, are based on six-coordinate and octahedral metal centers rather than the highly anisotropic low-coordinate metal ions. One of the main obstacles is the difficulty in maintaining the desired geometries within a framework during synthesis. In 2019, Huang *et al.* reported the first example of a 1D single ion magnets featuring four-coordinate metal centres which was constructed by a mixed benzimidazole–dicarboxylate strategy.[78] The slow magnetic relaxation can be observed under higher frequency (out-of-phase peak around 2280 Hz) because of the small easy-axis anisotropy (−12.8

Table 1 Structural and magnetic parameters of reported 1D SIM coordination polymers

Complex	Coordination number	Symmetry	D (cm^{-1})	U_{eff} (K)	Ref.
$[Co(btm)_2(SCN)_2 \cdot H_2O]_n$	6	O_h	93.9	45.4	71
$[Co(tdmmb)(bpe)][BF_4]_2 \cdot 3CH_3CN$	7	D_{5h}	21.7(7)	19.0	72
$[Co(L_{N_3O_2})]_6[Co^{III}(CN)_6]_4 \cdot 26H_2O$	7	D_{5h}	21.4(6)	9.1	73
$\{[Co(TPT)_{2/3}(H_2O)_4][CH_3COO]_2 \cdot (H_2O)_4\}_n$	6	O_h	47.7	6.91	74
$\{[Co_2(dmphen)_2(CPCA)_2]DMF\}_n$	6	D_{3h}	38.2(4)	9.2	75
$[Co(3\text{-}Hppt)_2(adip)(H_2O)_2] \cdot 2H_2O$	6	O_h	−33.9	29.08	76
$\{[Co(bimb)(H_2O)_4] \cdot (L_2) \cdot 2DMF\}_n$	6	O_h	57.5(2)	8.82	77
$[Co(SCA)_2(MBIm)_2]_n$	4	T_d	−12.8(7)	11.3	78
$[Co(H_3daps)(dca)] \cdot (MeOH)_2 \cdot (MeCN)$	7	D_{5h}	41.3	9.9	79
$[Co(btca)_{1/2}(mbpy)]_n$	5	D_{3h}	27.6	41.9	80
$[Co(pytpy)(DClbdc)]_n$	6	O_h	−59.5	27.3	81
$[Co(pytpy)(ndc)]_n$	6	O_h	−42.8	12.7	81
$[Co(pdms)(bpe)]_n$	4	T_d	−19	69.6	82
$\{[Co(pdms)(tpb)] \cdot H_2O \cdot tpb\}_n$	4	T_d	−33	76.6	82
$\{[Co(HL)(EtOH)_2](ClO_4)\}_n$	6	O_h	30.6	11.7	83

Abbreviations: **btm**, bis(1*H*-1,2,4triazol-1-yl)methane; **tdmmb**, 1,3,10,12-tetramethyl-1,2,11,12-tetraaza[3](2,6)-pyridino[3](2,9)-1,10-phenanthrolinophane-2,10-diene; **bpe**, 1,2-di(4pyridyl)ethane; **TPT**, 2,4,6-tris(4-pyridyl)-1,3,5-triazine; $\mathbf{L_{N_3O_2}}$, ligand derived from the and condensation of 2,6-diacetylpyridine with 3,6-dioxaoctane-1,8-diamine; **SCA**, succinicacid; **MBIm**, 5,6-dimethylbenzimidazole; **dmphen**, 2,9-dimethyl phenanthroline; $\mathbf{H_2CPCA}$, 3-(3-carboxyphenyl)-1*H*-pyrazole-5-carboxylic acid; 3-Hppt, 3-phenyl-5-(pyridin-3-yl)-1,2,4-triazole; $\mathbf{H_2adip}$, adipic acid; $\mathbf{H_2L1}$, 2,2′-[benzene-1,4-diylbis(methanediylsulfanediyl)]dibenzoic acid; **2,2′-bipy**, 2,2′-bipyridine; $\mathbf{H_2L2}$, 2,2′-(1,4-phenylenebis(methylene)) bis(sulfanediyl)dinicotinic acid; **bimb**, 1,4-bis(benzoimidazo-1-ly)benzene; $\mathbf{H_2salen}$, *N*,N_0-ethylenebis(salicylideneimine); **4,4-dmbipy**, 4,40-dimethyl-2,20-bipyridine; H_4**btca**, 1,2,4,5-benzenetetracarboxylic acid; **mbpy**, 4,4′-dimethyl-2,2′-bipyridyl; H_2**pdms**, 1,2-bis(methanesulfonamido) benzene; **tpb**, 1,2,4,5-tetra(4-pyridyl)benzene; H_2**L** = 2-[(*E*)-1H-imidazol-4-ylmethylidene]amino; H_4**daps**, 2,6-bis(1-salicyloylhydrazonoethyl) pyridine; **dca**, dicyanamide.

cm^{-1}) of the distorted tetrahedral Co^{II} centres. This result indicate that highly anisotropic Co^{II} centres are of great importance for designing high-performance 1D SIM coordination chains. Interestingly, Shao *et al.* recently isolated two rare Co(II) coordination polymers that exhibit a highly anisotropic four-coordinated Co center, using the Co(II) SIM, $(HNEt_3)_2[Co(pdms)_2]$, in conjunction with different linkers.[82] The assembly resulted in a 1D zig-zag chain with a ditopic ligand and a ribbon chain with a tetradentate linker (Fig. 3). Both experimental and theoretical analyses showed that the local Co(II) ion adopts a distorted tetrahedral geometry with quasi-C_{2v} symmetry, displaying uniaxial magnetization anisotropy along its C_2 axis. The magnitude of this anisotropy is significantly influenced by the N_{py}–Co–N_{py} bite angles. These findings exemplify the ability to manipulate magnetic anisotropy through topology control and the incorporation of highly anisotropic metal ions as nodes in coordination polymers.

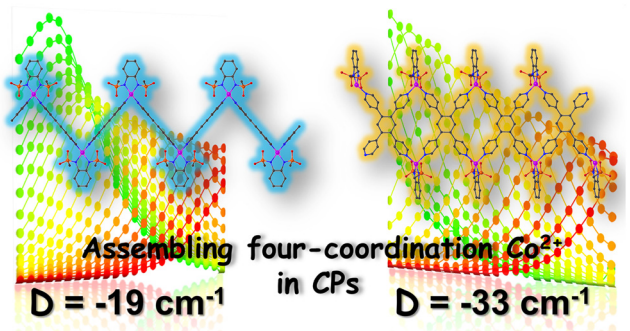

Fig. 3 Structures and ac magnetic behaviors of 1D zigzag chain and 1D ribbon compounds. This figure has been adapted from ref. 82 with permission from American Chemical Society, copyright 2023.

Efforts to manipulate magnetic anisotropy have primarily concentrated on finely adjusting the electronic configurations of metal centers within mononuclear complexes. This can be synthetically accomplished by altering coordination numbers, coordination atoms, and consequently, the molecular symmetry of the metal centers. Additionally, topology control represents a promising approach for tuning magnetic anisotropy, particularly in coordination polymers. Toward this end, we demonstrated the synthesis of two novel 1D cobalt(II) coordination polymers by combining a terpyridine derivative with two distinct dicarboxylates.[81] The chain topologies and magnetic anisotropy of the compounds were concurrently influenced by the choice of dicarboxylic acid bridging ligands. Magnetic and theoretical calculations confirmed that both compounds exhibited significant easy-axis magnetic anisotropy, attributed to the presence of very short axial Co–O bonds within the resulting chains. The compounds displayed slow magnetic relaxation behaviors under a direct current field, indicative of well-isolated Co^{2+} ions within and between the chains. These findings highlight a promising synthetic approach utilizing terpyridine and dicarboxylate ligands for tailoring the structure and magnetic properties of 1D compounds.

2D cobalt(II) SIMs

Since the discovery of graphene in 2004, extensive research has been conducted on 2D materials.[114] Various 2D MOFs have demonstrated potential for exfoliation into ultrathin

nanosheets, akin to graphene and other 2D materials, thereby offering unique layered structures with diverse technological applications.[115] These 2D structures exhibit intricate topological networks and entanglements, enhancing their appeal for applications. The design approach for 2D MOFs focuses on achieving specific topologies while incorporating essential properties such as porosity, optical, chiral, catalytic, electrical, and magnetic characteristics.[116] Notably, certain 2D MOFs exhibit magnetic properties like long-range ordering and spin crossover (SCO).[117] Despite these advancements, the development of 2D SIM-MOFs is still in its nascent stages.

In 2015, Andruh *et al.* first reported two 2D Co(II) coordination polymers constructed by angular and linear spacers *via* a node-and-spacer approach showing SIM property (Fig. 4).[84] Each cobalt center is connected to three other cobalt centers through bridging ligands, consisting of two azbbpy ligands and one 4,4′-bipy ligand. These ligands form distorted hexagonal meshes that interconnect the cobalt centers in the structure. The Co(II) ions within each mesh are spaced at distances of 14.02 and 11.48 Å. The intralayer intermetallic separations exhibit nearly identical values of 13.92 and 13.67 Å using the azbbpy and bpy spacers, respectively. The ac magnetic susceptibility measurements for the compounds show out-of-phase signals under 1000 Oe dc field with small energy barrier being 9.7 and 5.8 cm^{-1}, respectively. Then, a number of 2D cobalt(II) SIMs have been reported to showing varying structures and magnetic relaxation behaviors (Table 2).

Cano and colleagues have presented a series of 2D frameworks featuring a square grid topology constructed from singular Co(II) centers as nodes and elongated rod-like aromatic bipyridine ligands as linkers (Fig. 5a). This MOF showcases spacious square channels capable of accommodating a diverse array of guest organic molecules (Fig. 5b). The arrangement of cobalt(II) nodes within the square layers enhances magnetic properties by reducing intermolecular interactions among the cobalt(II) centers. Additionally, the SIM behavior was observed to vary depending on the nature of the aromatic guest molecules. Wang and co-workers presented two cobalt(II) MOFs featuring 2-fold vertically interpenetrated (4,4) grids, synthesized under distinct solvent conditions (Fig. 6). Despite their structural similarities, subtle variations in guest molecules induce changes in the coordination environments of the Co^{II} centers, intergrid supramolecular interactions, and dihedral angles of the interpenetrated grids. These structural modifications result in altered magnetic properties, particularly evident in the dynamic magnetic behavior at low temperatures. Both compounds demonstrate slow magnetic relaxation in the presence of an external field. Notably, the Co-MOF hosting DMF exhibits a significantly higher estimated energy barrier compared to that hosting MeOH, leading to markedly slower magnetic relaxation. The divergent magnetic behaviors observed in the two MOFs highlight the impact of host–guest interactions on the tunability of SIM property within MOFs, underscoring the significant influence of guest molecules on the magnetic properties of MOF-based SIMs.

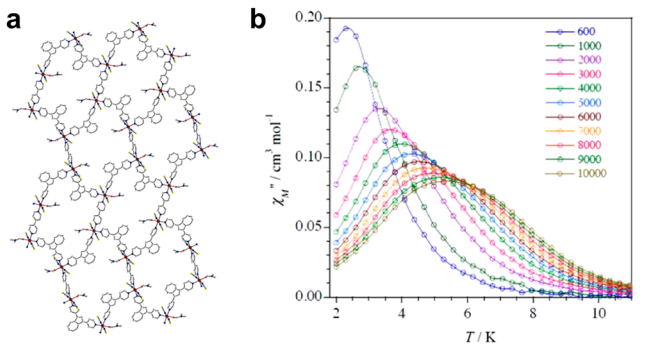

Fig. 4 (a) Crystal structure of $[Co(azbbpy)(4,4'\text{-bipy})_{0.5}(DMF)(NCS)_2]\cdot MeOH$ and (b) its frequency dependence of the out-of-phase ac susceptibilities. This figure has been adapted from ref. 84 with permission from American Chemical Society, copyright 2014.

The use of cyanometallates as building blocks proved to be highly effective in the synthetic strategy, leading to the creation of a wide range of magnetic materials with unique properties.[118,119] These include high-temperature magnetic ordering, SCO, photo-magnetism, SMMs, single-chain magnets (SCMs), and more.[120–124] Therefore, it's highly promising to prepare SIM-MOF through diamagnetic cyanometallates.[125] In 2017, Wang *et al.* synthesized a 2D honeycomb coordination polymer, Co-TODA, using the pentagonal-bipyramidal Co^{II} precursor, $[Co(TODA)]^{2+}$, and a diamagnetic $[Co^{III}(CN)_6]^{3-}$ unit (Fig. 7).[96] They found that the Co^{II} centers in the compound exhibited easy-plane magnetic anisotropy with a D value of 29.9 cm^{-1}. Furthermore, they observed field-induced slow magnetic relaxation in Co-TODA, making it a rare example of a 2D SIM based on $[Co^{III}(CN)_6]^{3-}$. This study demonstrates that combining diamagnetic cyanometallates with Co^{II} precursors is an effective strategy for designing and synthesizing SIM-MOFs. In order to gain in-depth understanding of the ZFS parameters of Co-TODA, Xue and co-workers utilized a combination of far-IR magneto-spectroscopy (FIRMS), variable-temperature (VT) HFEPR, and inelastic neutron scattering (INS) techniques to characterize the compound.[126] Notably, EPR spectroscopy can provide detailed information on its electronic structure, making EPR spectroscopy an invaluable tool in the study of the relationship between structure and magnetic anisotropy. In particular, HF-EPR is particularly successful in determining g-matrix parameters and deliver highly accurate values of the ZFS tensor for Co^{II} complexes. The results from both methods indicated that Co-TODA exhibits easy-plane magnetic anisotropy with a value of D between +38.0(1.0) and +40.2(1.0) cm^{-1}. Pulsed X-band EPR studies were also conducted to investigate the relaxation of Co^{2+} ions from the M_S = +1/2 to −1/2 state in the ground Kramers doublet (KD), providing information on spin–lattice and spin–spin relaxation times. This study serves as a valuable example of how spectroscopic techniques and computational methods can be combined to determine the magnetic and phonon properties of a MOF.

The coordination of a cobalt(II) salt with two gold cyanide anions and ancillary ligands such as DMF, DMSO, Py, and

Table 2 Structural and magnetic parameters of reported 2D SIM coordination polymers

Complexes	Coordination number	Symmetry	D (cm^{-1})	U_{eff} (K)	Ref.
$[Co(azbbpy)(4,4'\text{-}bipy)_{0.5}(DMF)(NCS)_2]\cdot MeOH$	6	O_h	—	13.9	84
$[Co(azbbpy)(bpe)_{0.5}(DMF)(NCS)_2]\cdot 0.25H_2O$	6	O_h	—	8.4	84
$[Co(ppad)_2]_n$	6	O_h	+76	16.4	85
$[Co(dca)_2(atz)_2]_n$	6	O_h	—	7.3	86
$\{[Co(bmzbc)_2]\cdot 2DMF\}_n$	6	O_h	+62.6	11.8	87
$[Co(L)_2(SCN)_2\cdot 2(CH_3CN)\cdot 2(dmf)]_n$	6	O_h	+41.6	36.9	88
$\{[Co(3,3'\text{-}Hbpt)_2(SCN)_2]\cdot 2H_2O\}_n$	6	O_h	+70.1	33.5	89
$[Co(dca)_2(bim)_2]_n$	6	O_h	+74.3	7.7	89
$[Co(dca)_2(bmim)_2]_n$	6	O_h	+75.8	19.9	90
$[Co(bpeb)_2(NCS)_2]\cdot nG$ (G = DCB)	6	O_h	+64.9(9)	45.1	91
$[Co(bpeb)_2(NCS)_2]\cdot nG$ (G = TAN)	6	O_h	+67.1(9)	24.6	91
$[Co(bpeb)_2(NCS)_2]\cdot nG$ (G = TOL)	6	O_h	+84.4(4)	16.56	91
$[Co(bpeb)_2(NCS)_2]\cdot nG$ (G = PYR)	6	O_h	+70.3(9)	30.24	91
$[Co(bmzbc)_2(1,2\text{-}etdio)]_n$	6	O_h	—	16.7	92
$[Co(bmzbc)_2(Hbmzbc)]_n$	6	O_h	—	31.2	92
$\{[Co(HL)(bpy)(H_2O)_2]\cdot DMF\}_n$	6	O_h	−0.071	13.9	93
$\{[Co(HL)(bpe)]\cdot 0.5bpe\}_n$	6	O_h	−0.076	8.7	93
$[Co(\mu\text{-}6ani)_2]\cdot H_2O$	6	O_h	+28	18.7	94
$\{[Co(TPT)_{2/3}(H_2O)_4][CH_3COO]_2\cdot(H_2O)_4\}_n$	6	O_h	+47.7	6.912	95
$[Co^{III}(CN)_6]_2[Co^{II}(TODA)]_3\cdot 9H_2O$	7	D_{5h}	+29.9	16	96
$[Co(bpg)_2(SCN)_2]\cdot 3MeOH$	6	O_h	+64.2	5.0	97
$[Co(bpg)_2(SCN)_2]\cdot 2DMF$	6	O_h	+67.5	15.3	97
$[Co(1,4\text{-}bimb)_{0.5}(5\text{-}aip)(H_2O)]_n$	6	O_h	—	4.9	98
$[Co(dps)_2Cl_2]_n$ (α)	6	O_h	27.2	12.4	99
$[Co(dps)_2Br_2]_n$	6	O_h	28.0	27.1	99
$[Co(dps)_2(H_2O)_2\cdot I_2\cdot(H_2O)_4]_n$	6	O_h	9.5	28.8	99
$\{Co(DMSO)_2[Au(CN)_2]_2\}_n$	6	O_h	+68	22.1	100
$\{Co(DMF)_2[Au(CN)_2]_2\}_n$	6	O_h	+90	18.5	100
$\{Co(PY)_2[Au(CN)_2]_2\}_n$	6	O_h	+75	22.0	100
$\{Co(PyPhCO)_2[Au(CN)_2]_2\}_n$	6	O_h	+80	15.9	100
$[Co(m\text{-}NPy_3)(TPA)0.5Cl\cdot CH_3OH]_n$	6	O_h	—	9.89	101
$\{[Co(IPEH)_2(SCN)_2]\cdot H_2O\}_n$	6	O_h	89.3	6.5	102
$[Co(Hbic)_2]_\alpha$	4	T_d	−20.4	24.9	103
$[Co(Hbic)_2]_\beta$	4	T_d	−14.6	4.3	103
$\{Co_2(DClQ)_4(tpb)\}_n$	6	O_h	−46.0	23.5	104
$[Co(dps)_2Cl_2]_n$ (β)	6	O_h	104.57	28.56	105
$\{[Co(H_2tbca)(bpb)(H_2O)_2]\cdot bpb\}_n$	6	O_h	62.1	31.8	106
$\{[Co(Hbic)(H_2O)]\cdot 4H_2O\}_n$	6	O_h	87.1	45.2	107

Abbreviations: **azbbpy**, 1,3-bis(4-pyridyl)azulene; **4,4′bipy**, 4,4′-bipyridyl; **bpe**, 1,2-bis(4-pyridyl)ethylene; **Ppad**, N_3-(3-pyridoyl)-3-pyridinecarboxamidrazone; **dca**, dicyanamide; **atz**, 2-amino1,3,5-triazine; **bmzbc**$^-$, 4-(benzimidazole-1-yl)benzoate; **L**, 4′-(4-methoxyphenyl)-4,2′:6′,4″-terpyridine; **3,3′-Hbpt**, 1*H*-3-(3-pyridyl)-5-(30-pyridyl)-1,2,4-triazole; **dca**, dicyanamide; **bim**, 1-benzylimidazole; **bmim**, 1-benzyl-2-methyl-imidazole; 6ani, 6-aminonicotinate; **TPT**, 2,4,6-tris(4-pyridyl)-1,3,5-triazine; **bpg**, *meso*-α,β-bi(4-pyridyl) glycol; **1,2-etdio**, 1,2-ethanediol; **Hbmzbc**, 4-(benzimidazole-1-yl)benzoic acid; **6ani**, 6-aminonicotinate; **bpg**, *meso*-α,β-bi(4-pyridyl) glycol; **dps**, 4,4′-dipyridyl sulfide; PyPhCO, benzoylpyridine; **TPA**, bidentate terephthalic acid; ***m*-NPy3**, tris(4-(pyridine-3-yl)phenyl)amine ligand; **IPEH**, (1*E*,2*E*)-1,2-bis(1-(4-(1*H*-imidazol-1-yl)phenyl)ethylidene)hydrazine; **tpb**, 1,2,4,5tetra(4-pyridyl)benzene; **DClQ**, (5,7-dichloro-8-hydroxyquinoline; H_4**btca**, 1,2,4,5-benzenetetracarboxylic acid; **mbpy**, 4,4′-dimethyl-2,2′-bipyridyl; H_2**bic**, 1*H*-benzimidazole-5-carboxylic acid.

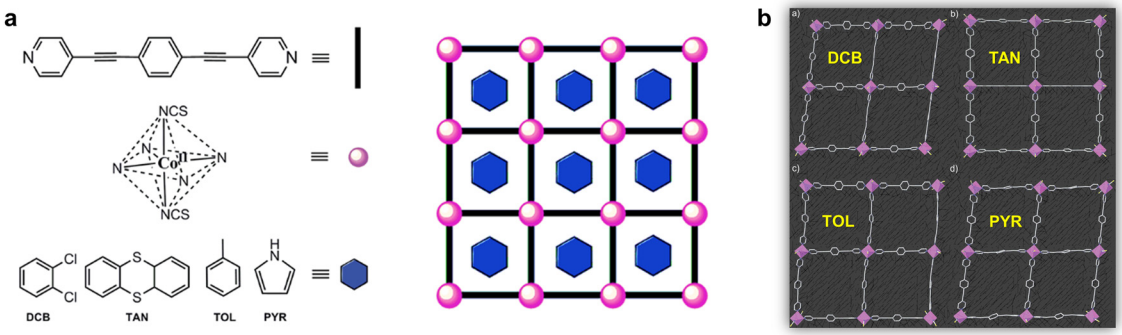

Fig. 5 (a) Approach to ligand design for Co(II) SIM-MOFs aimed at magnetic detection of aromatic compounds. (b) Structures of the Co(II) SIM-MOFs hosting DCB, TAN, TOL, and PYR.[91] This figure has been adapted from ref. 91 with permission from Royal Society of Chemistry, copyright 2016.

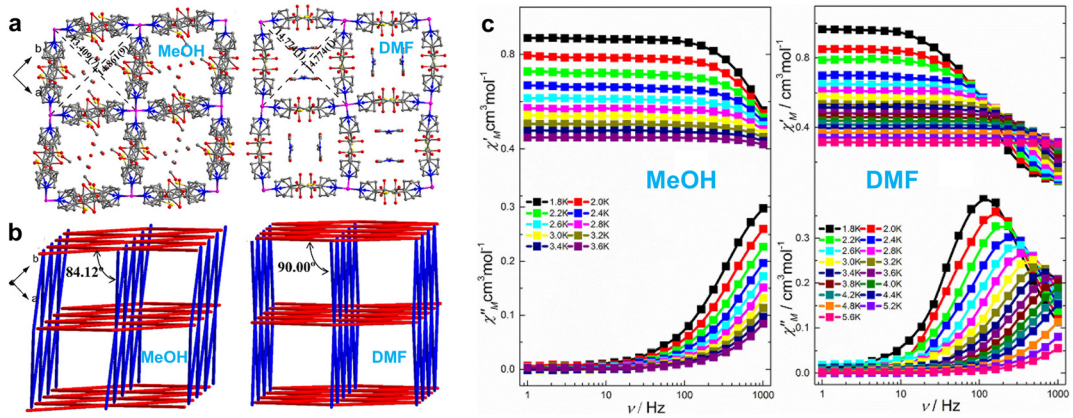

Fig. 6 (a) 1D channels along the *c*-axis in the Co(II) MOFs, $[Co(bpg)_2(SCN)_2]\cdot sol$; (b) 2-fold interpenetrated 3D frameworks of the Co(II) MOFs; (c) frequency-dependent ac susceptibilities for the Co(II) MOFs.[97] This figure has been reproduced from ref. 97 with permission from American Chemical Society, copyright 2018.

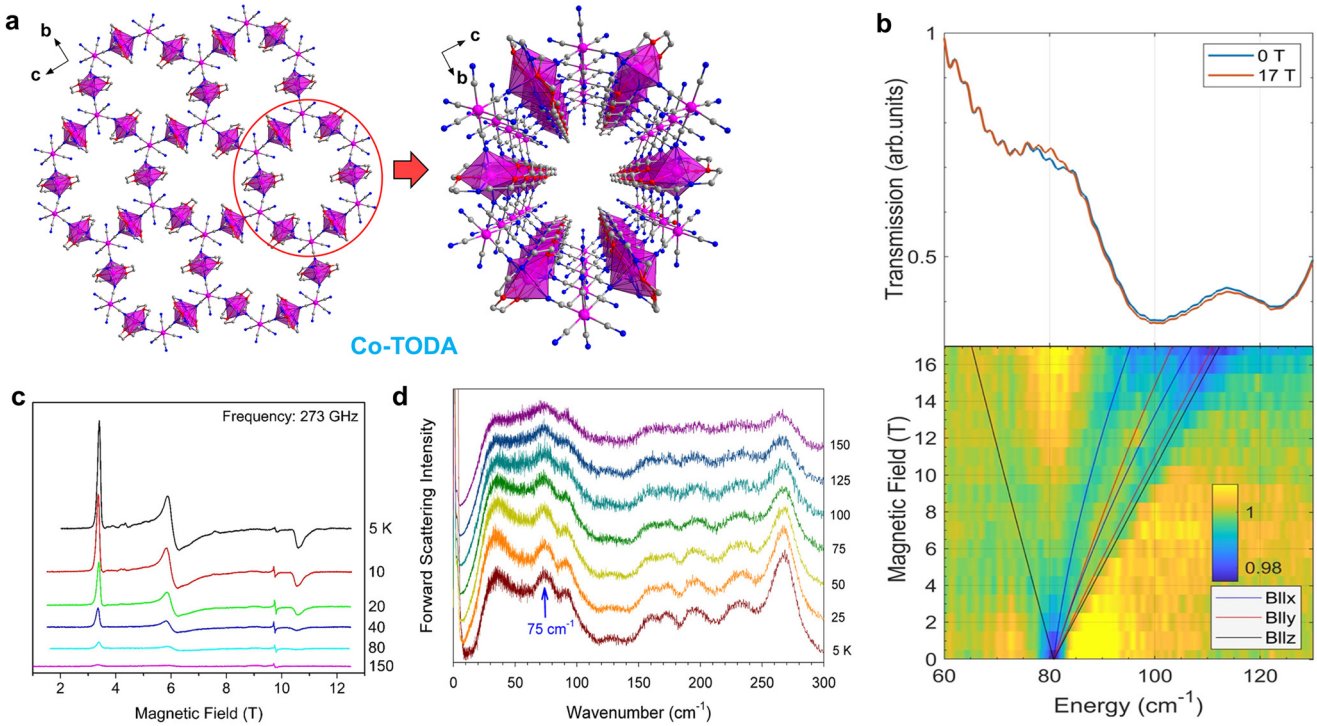

Fig. 7 (a) 2D honeycomb layer structure of **Co-TODA** and the hexagonal 1D channel along the *a* axis. This figure has been reproduced from ref. 96 with permission from American Chemical Society, copyright 2017. (b) Transmittance line plot of FIRMS data at 5.3(3) K2D FIRMS plot; (c) VT HFEPR; (d) Bose-corrected INS spectra collected at VISION.[126] This figure has been reproduced from ref. 126 with permission from American Chemical Society, copyright 2022.

PyPhCO resulted in the formation of structurally varying 2D cobalt(II) MOFs. The cobalt center has a slightly tetragonally distorted coordination environment with the ancillary ligands occupying the axial positions. These ligands are positioned to penetrate the cavities of adjacent layers. Through analysis of DC magnetic properties, HFEPR, and FIRMS measurements, and *ab initio* calculations, it is revealed that the cobalt ions in the compounds exhibit significant, positive, and diverse D values exceeding +70 cm^{-1}. The experimental D values align with those derived from *ab initio* calculations, underscoring the influential role of Au(I) in determining the Co(II) ions' anisotropy. The four MOFs exhibit field-induced slow magnetic relaxation primarily through a Raman mechanism, indicating 2D SIM of the four MOFs. The lack of a clear correlation between the anisotropy order and Co(II)···Co(II) distances with the empirical U_{eff} parameter suggests that factors other than these, such as the flexibility of the axial ligands, may play a significant role in the observed rapid relaxation in these complexes.

Compared to 2D MOFs with singular properties, these particular materials have the potential to expand into diverse applications through the utilization of bifunctional ligands and distinctive assembly methods. The precise arrangement of building blocks, comprising 'functional' metal centers and 'functional' organic bridging ligands, plays a vital role in the construction of these materials. To prepare multifunctional SIM-MOF materials, Dou *et al.* synthesized two cobalt coordination compounds using a flexible phenolic multi-carboxylic acid ligand.[93] Both compounds, forming 2D cobalt MOFs, display simple sql networks with distinct arrangements. It is worth noting that these compounds display field-induced single-ion relaxation magnetization and show exceptional catalytic activity in benzylic C–H oxidation reactions. This result indicates an inorganic and organic applications *via* a MOF. Recently, we reported a 2D proton-conductive Co(II) SIM-MOF was synthesized hydrothermally using a ditopic organic ligand.[107] In this material, the Co^{2+} ions were effectively isolated within the framework, while hydrogen-bonded water tetramers were identified within porous channels, creating 1D pathways for proton transport. This resulted in a notable proton conductivity of 1.6×10^{-4} Scm^{-1} at 300 K under 95% relative humidity. Magnetic studies, in conjunction with theoretical calculations, unveiled a significant easy-plane magnetic anisotropy of the Co^{2+} ions in distorted octahedral geometry, with computed and experimental D values of 109.3 and 87.1 cm^{-1}, respectively. Furthermore, the Co(II) MOF displays field-induced slow magnetic relaxation at very low temperatures, with an U_{eff} of 45.2 cm^{-1}. However, the bifunctionality has no coupling between each other in these reported systems, indicating a major challenge in designing synergetic SIM property with other physical properties.

3D cobalt(II) SIMs

3D MOFs are constructed by the self-assembly of inorganic ions/clusters and organic linkers, forming porous framework structures with diverse topologies. These MOFs are widely utilized in gas storage, separation, magnetism, catalysis, and sensing due to their exceptional porosity. A novel subgroup, termed SIM-MOFs, showcases highly anisotropic metal nodes and organic linkers, holding promise as new framework magnets. The pronounced porosity of SIM-MOFs allows for the inclusion of diverse guest molecules, facilitating the manipulation of magnetization dynamics. The shape, size, and hydrogen-bonding characteristics of guest molecules have the potential to significantly influence SIM behaviors. To date, reported 3D SIM-MOFs are very rare while their SIM properties are worse.[108–110]

In 2016, Liu *et al.* reported a MOF features a 3D chiral framework with 2-fold interpenetrating **qtz** topology made up of completely achiral ligands (Fig. 8).[108] Within the framework, the Co^{2+} ions are spaced apart by the long organic linkers, forming distinct networks. Magnetic studies revealed slow magnetic relaxation induced by the single-ion magnetic anisotropy of the Co^{2+} ions, with a U_{eff} of 16.8(3) K. This compound represents the initial instance of a 3D framework constructed from Co^{II} SIMs as nodes. Later, Murugesu's group successfully synthesized a 3D Co^{II} MOF using an innovative crystalline sponge technique.[109] This MOF demonstrates unique SIM behavior when subjected to static dc fields. In addition, they observed distinct magnetic properties in two other related compounds due to subtle changes in the coordination geometry of the Co^{2+} ions within the MOF. Magnetic analysis demonstrated the presence of unquenched orbital angular momentum in the compounds, leading to pronounced magnetic anisotropy, a finding corroborated by CASSCF-type calculations. The discovery of this SIM behavior in a crystalline sponge presents new avenues for future research on guest encapsulation, where both diamagnetic and paramagnetic guests can influence the overall magnetic anisotropy and relaxation dynamics.

Interpenetration isomerism is a fascinating phenomenon in the fields of supramolecular chemistry, coordination chemistry, and crystal engineering.[127] Interpenetrated MOFs, which are made up of two or more independent frameworks interlocked with each other, have been extensively studied. MOF or supramolecular isomers are also of great interest as they provide a valuable opportunity to study self-assembly and crystal growth processes, as well as to explore structure–performance relationships. However, the magnetic anisotropy and slow magnetic relaxation behaviors of MOF isomers, especially rare interpenetrated MOF isomers, have not been thoroughly investigated. This presents a promising avenue for future research and opens up new possibilities for the design and synthesis of SIM isomers. Wei *et al.* conducted a study on the structure and magnetic properties of two Co^{II} coordination compounds using a benzimidazole carboxylic ligand with dual functionality (Fig. 9).[103] The compounds exhibit interpenetrated isomers with different levels of interpenetration and distinct framework structures (Fig. 9a and b). Magnetic studies revealed notable magnetic anisotropy of the Co(II) ions and distinct slow magnetic relaxation under applied dc field in these compounds (Fig. 9c). These compounds are the first example of MOF isomers exhibiting distinct field-induced SIM behaviors, suggesting that MOF isomers offer a promising opportunity to manipulate slow magnetic relaxation behavior and magnetic anisotropy.

Conclusions and perspective

In conclusion, magnetic metal coordination polymers present a promising avenue for advancing molecular nanomagnet development. In contrast to inorganic solids, these polymers offer distinct advantages, including tailored structures with regulated porosity and opportunities for subsequent chemical adjustments. This review outlines recent advancements in Co(II)-based coordination polymers displaying SIM characteristics. It is anticipated that investigations into SIM behaviors of Co(II)-based coordination polymers may pave the way for novel material innovations with potential applications in areas such as magnetic sensors, data storage and quantum

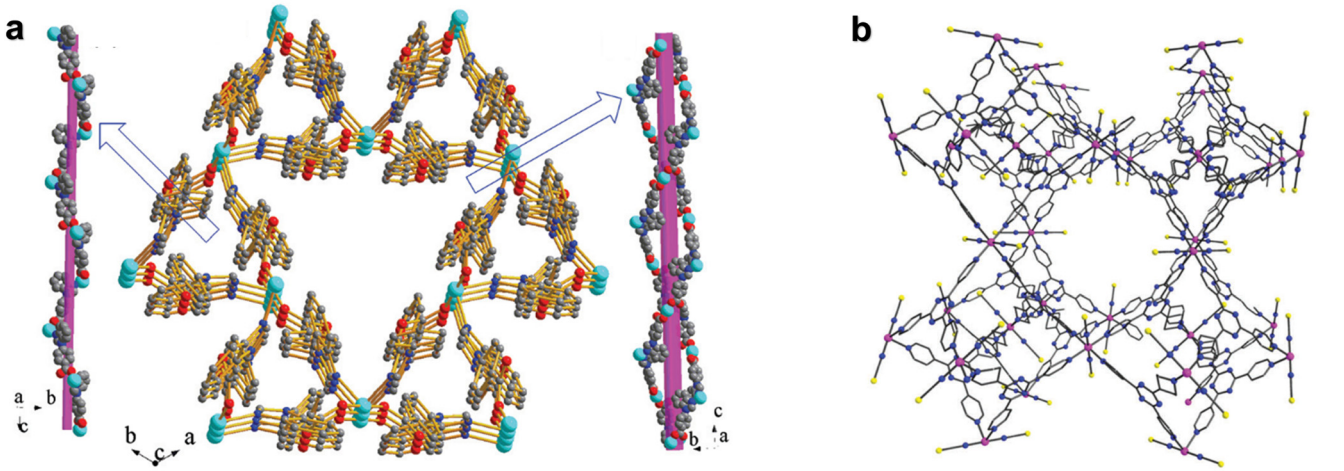

Fig. 8 (a) 3D framework and the left-handed helix in $[Co(bmzbc)_2(1,2\text{-etdio})]_n$;[108] (b) large pore dimensions of the 3D network of $\{[(Co(NCS)_2)_3(k^3\text{-}TPT)_4]a(H_2O)_b(MeOH)\}_n$.[109] This figure has been reproduced from ref. 109 with permission from Royal Society of Chemistry, copyright 2017.

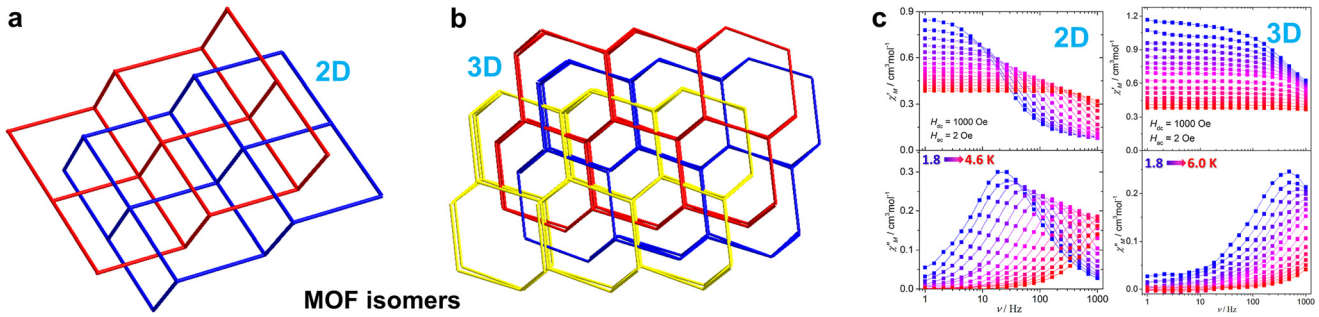

Fig. 9 (a) The two-fold interpenetrated **sql** nets and (b) three-fold interpenetrated **dia** nets of two Co(II) MOF isomers; (c) ac magnetic susceptibilities for the Co(II) MOF isomers.[103] This figure has been reproduced from ref. 103 with permission from Royal Society of Chemistry, copyright 2020.

computing. Despite the remarkable progresses that have been made since the first SIM coordination polymers, there still remains challenges and plenty of rooms for advancing future research of Co(II) SIM coordination polymers.

(1) High-performance Co(II) SIM coordination polymers. The quenching of first-order orbital angular momentum has been shown in common five- and six-coordinate complexes, with the observed zero-field splitting arising from second-order spin–orbit coupling. However, low-coordinate geometries have attracted attention due to their promotion of degenerate ground state orbitals, leading to minimal quenching of orbital angular momentum and consequently first-order spin–orbit coupling.[128–130] To achieve high-performance coordination polymers of Co(II) SIMs, it is crucial to incorporate highly anisotropic low-coordinated metal centers in the polymers.

(2) Multifunctional Co(II) SIM-MOFs. Over the past few decades, researchers have shown great interest in multifunctional molecular materials, as they hold the promise of generating new physical phenomena and applications.[131] There are a number of multifunctional SMMs systems have been reported, such as SMM dielectrics, SMM ferroelectric, SMM-SCO materials, SMM conductors, *etc.*[132–134] MOFs, with their customizable structures and adaptable functionalities, serve as a versatile platform for exploring multifunctional molecular magnetic materials. A number of magnetic multifunctional MOFs have been reported.[67] Therefore, it's a great chance to develop multifunctional Co(II) SIM-MOFs, such as proton-conducting Co(II) SIM-MOFs.[107] However, such molecular systems are extremely rare.

(3) Dynamic Co(II) SIM coordination polymers. Dynamic molecular crystals with switchable physical properties are of great interest for developing innovative functional materials and gaining profound insights into physical properties.[135] The dynamic transformation processes can trigger structural changes in coordination polymers, resulting in a material that exhibits reversible structural alterations in response to external stimuli.[136,137] The magnitude and directionality of these structural phase transitions play a crucial role in determining the intrinsic electrical conductivity, magnetism, and optical properties of the materials.[138] Therefore, there is a compelling opportunity to engineer dynamic SIMs coordination polymers that exhibit dynamic changes in their crystalline network upon exposure to external stimuli. To date, there have been no reports on related dynamic SIM coordination polymers.

Overall, research on Co(II) SIM CPs has entered a phase of rapid advancement, yet significant strides and directions are still required to achieve high-performance SIM CPs. The ongoing efforts and advancements in Co(II) SIM CPs are driving the exploration of innovative molecular nanomagnets. Looking ahead, substantial work lies ahead, underscoring the promising trajectory of cobalt SIM CPs.

Conflicts of interest

There are no conflicts to declare.

Acknowledgements

We acknowledge the Chutian Scholars Program of Hubei Province, Huanggang Normal University (2042021033, 202210204) and the Hubei Provincial Natural Science Foundation (2023AFB010).

Notes and references

1 R. Sessoli, D. Gatteschi, A. Caneschi and M. A. Novak, *Nature*, 1993, **365**, 141–143.
2 D. Gatteschi and R. Sessoli, *Angew. Chem., Int. Ed.*, 2003, **42**, 268–297.
3 M. N. Leuenberger and D. Loss, *Nature*, 2001, **410**, 789–793.
4 L. Bogani and W. Wernsdorfer, *Nat. Mater.*, 2008, **7**, 179–186.
5 E. Coronado, *Nat. Rev. Mater.*, 2020, **5**, 87–104.
6 D. N. Woodruff, R. E. Winpenny and R. A. Layfield, *Chem. Rev.*, 2013, **113**, 5110–5148.
7 F.-S. Guo, A. K. Bar and R. A. Layfield, *Chem. Rev.*, 2019, **119**, 8479–8505.
8 J.-L. Liu, Y.-C. Chen and M.-L. Tong, *Chem. Soc. Rev.*, 2018, **47**, 2431–2453.
9 J. Ferrando-Soria, J. Vallejo, M. Castellano, J. Martínez-Lillo and E. Pardo, *Coord. Chem. Rev.*, 2017, **339**, 17–103.
10 D. Shao and X.-Y. Wang, *Chin. J. Chem.*, 2020, **38**, 1005–1018.
11 C. A. P. Goodwin, F. Ortu, D. Reta, N. F. Chilton and D. P. Mills, *Nature*, 2017, **548**, 439–442.
12 F.-S. Guo, B. M. Day, Y.-C. Chen, M.-L. Tong, A. Mansikkamäki and R. A. Layfield, *Science*, 2018, **362**, 1400–1403.
13 P. C. Bunting, M. Atanasov, E. Damgaard-Møller, M. Perfetti, I. Crassee, M. Orlita, J. Overgaard, J. V. Slageren, F. Neese and J. R. Long, *Science*, 2018, **362**, eaat7319.
14 P. Abbasi, K. Quinn, D. I. Alexandropoulos, M. Damjanović, W. Wernsdorfer, A. Escuer, J. Mayans, M. Pilkington and T. C. Stamatatos, *J. Am. Chem. Soc.*, 2017, **139**, 15644–15647.
15 D. E. Freedman, W. H. Harman, T. D. Harris, G. J. Long, C. J. Chang and J. R. Long, *J. Am. Chem. Soc.*, 2010, **132**, 1224–1225.
16 S.-D. Jiang, B.-W. Wang, H.-L. Sun, Z.-M. Wang and S. Gao, *J. Am. Chem. Soc.*, 2011, **133**, 4730–4733.
17 M. Feng and M.-L. Tong, *Chem. – Eur. J.*, 2018, **24**, 7574–7594.
18 G. A. Craig and M. Murrie, *Chem. Soc. Rev.*, 2015, **44**, 2135–2147.
19 Y.-S. Meng, S.-D. Jiang, B.-W. Wang and S. Gao, *Acc. Chem. Res.*, 2016, **49**, 2381–2389.
20 C. Wang, Y.-S. Meng, S.-D. Jiang, B.-W. Wang and S. Gao, *Sci. China: Chem.*, 2023, **66**, 683–702.
21 Y.-F. Deng, T. Han, Z.-X. Wang, Z.-W. Ouyang, B. Yin, Z.-P. Zheng, J. Krzystek and Y.-Z. Zheng, *Chem. Commun.*, 2015, **51**, 17688–17691.
22 B. Zhang, Y. Zhou, H.-Y. Huang, X.-L. Zhang, Y. Xiang, Y. Shi, C. Zhang, A. Yuan, X. Cai, L. Chen, Y.-Q. Zhang and Z.-B. Hu, *Inorg. Chem. Front.*, 2024, **11**, 2648–2660.
23 J. Vallejo, A. Pascual-Alvarez, J. Cano, I. Castro, M. Julve, F. Lloret, J. Krzystek, G. D. Munno, D. Armentano, W. Wernsdorfer, R. Ruiz-Garcia and E. Pardo, *Angew. Chem., Int. Ed.*, 2013, **52**, 14075–14079.
24 Y. Zhou, P. Tan, R. Jing, M. Liu, Y. Xiang, A. Yuan, S.-C. Luo, H.-H. Cui, L.-X. Shi and L. Chen, *Cryst. Growth Des.*, 2022, **22**, 6792–6800.
25 M. Liu, Y. Yang, R. Jing, S. Zheng, A. Yuan, Z. Wang, S.-C. Luo, X. Liu, H.-H. Cui, Z.-W. Ouyang and L. Chen, *Dalton Trans.*, 2022, **51**, 8382.
26 G. Yi, C. Zhang, W. Zhao, H. Cui, L. Chen, Z. Wang, X.-T. Chen, A. Yuan, Y.-Z. Liu and Z.-W. Ouyang, *Dalton Trans.*, 2020, **49**, 7620.
27 Y. Zhou, R.-Z. Yao, X. Cai, Z. Wang, P. Cen, Y. Yang, A. Yuan, Y. Tang, X.-Y. Chen, S. Zhang, Z.-W. Ouyang and L. Chen, *J. Mol. Struct.*, 2023, **1294**, 136391.
28 D.-S. Tu, D. Shao, H. Yan and C.-S. Lu, *Chem. Commun.*, 2016, **52**, 14326.
29 D. Shao, S.-L. Zhang, L. Shi, Y.-Q. Zhang and X.-Y. Wang, *Inorg. Chem.*, 2016, **55**, 10859–10869.
30 X.-C. Huang, C. Zhou, D. Shao and X.-Y. Wang, *Inorg. Chem.*, 2014, **53**, 12671–12673.
31 J. Xiang, J.-J. Liu, X.-X. Chen, L.-H. Jia, F. Yu, B.-W. Wang, S. Gao and T.-C. Lau, *Chem. Commun.*, 2017, **53**, 1474.
32 J. M. Zadrozny, D. J. Xiao, M. Atanasov, G. J. Long, F. Grandjean, F. Neese and J. R. Long, *Nat. Chem.*, 2013, **5**, 577–581.
33 K. E. R. Marriott, L. Bhaskaran, C. Wilson, M. Medarde, S. T. Ochsenbein, S. Hill and M. Murrie, *Chem. Sci.*, 2015, **6**, 6825–6828.
34 D. Lomjansky, J. Moncoĺ, C. Rajnák, J. Titiš and R. Boča, *Chem. Commun.*, 2017, **53**, 6930.
35 R. Boča, C. Rajnák, J. Titiš and D. Valigura, *Inorg. Chem.*, 2017, **56**, 1478–1482.
36 D. Shao, F.-X. Xu, L. Yin, H.-Q. Li, Y.-C. Sun, Z.-W. Ouyang, Z.-X. Wang, Y.-Q. Zhang and X.-Y. Wang, *Chin. J. Chem.*, 2022, **40**, 2193–2202.
37 D. Shao, Y. Zhou, X. Yang, J. Yue, S. Ming, X.-Q. Wei and Z. Tian, *Dalton Trans.*, 2022, **51**, 18514–18519.
38 D. Shao, S. Moorthy, Y. Zhou, S.-T. Wu, J.-Y. Zhu, J. Yang, D.-Q. Wu, Z. Tian and S. K. Singh, *Dalton Trans.*, 2022, **51**, 9357–9368.
39 D. Shao, P. Peng, M. You, L.-F. Shen, S.-Y. She, Y.-Q. Zhang and Z. Tian, *Inorg. Chem.*, 2022, **61**, 3754–3762.
40 D. Shao, S.-Y. She, L.-F. Shen, X. Yang and Z. Tian, *Polyhedron*, 2022, **213**, 115614.

41 X.-J. Xiong, Y.-L. Zhang, X.-C. Huang, G. Liu and D. Shao, *Polyhedron*, 2023, **243**, 116567.
42 D.-Q. Wu, S. Moorthy, S.-Y. Yang, Q. Zhang, J. Yang, B. Zhai, S. K. Singh and D. Shao, *Dalton Trans.*, 2023, **52**, 16197–16205.
43 D. Shao, Z. Ruan, J. Dong, L. Huang, M. You, J. Yang and L. Shi, *J. Mol. Struct.*, 2023, **1294**, 136548.
44 X.-Q. Wei, Y. Wan, W.-J. Tang, J. Dong, L. Huang, J. Yang, X.-C. Huang and D. Shao, *J. Mol. Struct.*, 2024, **1305**, 137823.
45 G. Lococciolo, S. K. Gupta, S. Dechert, S. Demeshko, C. Duboc, M. Atanasov, F. Neese and F. Meyer, *Inorg. Chem.*, 2024, **63**, 5652–5663.
46 B. Yao, M. K. Singh, Y.-F. Deng, Y.-N. Wang, K. R. Dunbar and Y.-Z. Zhang, *Inorg. Chem.*, 2020, **59**, 8505–8513.
47 I. Bhowmick, A. J. Roehl, J. R. Neilson, A. K. Rappe and M. P. Shores, *Chem. Sci.*, 2018, **9**, 6564–6571.
48 R. Khurana and M. E. Ali, *Inorg. Chem.*, 2022, **61**, 15335–15345.
49 T. T. da Cunha, V. M. M. Barbosa, W. X. C. Oliveira, E. F. Pedroso, D. M. A. García, W. C. Nunes and C. L. M. Pereira, *Inorg. Chem.*, 2020, **59**, 12983–12987.
50 H. Kato, Y. Horii, M. Noguchi, H. Fujimori and T. Kajiwara, *Chem. Commun.*, 2023, **59**, 14587–14590.
51 P. K. Sahu, R. Kharel, S. Shome, S. Goswami and S. Konar, *Coord. Chem. Rev.*, 2023, **475**, 214871.
52 X.-N. Yao, J.-Z. Du, Y.-Q. Zhang, X.-B. Leng, M.-W. Yang, S.-D. Jiang, Z.-X. Wang, Z.-W. Ouyang, L. Deng, B.-W. Wang and S. Gao, *J. Am. Chem. Soc.*, 2017, **139**, 373–380.
53 J. Jung, C. M. Legendre, S. Demeshko, R. Herbst-Irmer and D. Stalke, *Inorg. Chem.*, 2021, **60**, 9580–9588.
54 S. K. Gupta, S. V. Rao, S. Demeshko, S. Dechert, E. Bill, M. Atanasov, F. Neese and F. Meyer, *Chem. Sci.*, 2023, **14**, 6355–6374.
55 M. Cirulli, E. Salvadori, Z.-H. Zhang, M. Dommett, F. Tuna, H. Bamberger, J. E. M. Lewis, A. Kaur, G. J. Tizzard, J. V. Slageren, R. Crespo-Otero, S. M. Goldup and M. M. Roessler, *Angew. Chem., Int. Ed.*, 2021, **60**, 16051–16058.
56 F. Shao, B. Cahier, E. Rivière, R. Guillot, N. Guihéry, V. E. Campbell and T. Mallah, *Inorg. Chem.*, 2017, **56**, 1104–1111.
57 A. Landart-Gereka, M. M. Quesada-Moreno, M. A. Palacios, I. F. Díaz-Ortega, H. Nojiri, M. Ozerov, J. Krzystekd and E. Colacio, *Chem. Commun.*, 2023, **59**, 952–955.
58 H.-H. Cui, H.-J. Xu, T. Zhang, S. Luo, W. Tong, M. Wang, J. Wang, L. Chen and Y. Tang, *Dalton Trans.*, 2023, **52**, 7718–7723.
59 D. Shao, L. Shi, L. Yin, B.-L. Wang, Z.-X. Wang, Y.-Q. Zhang and Xin-Yi Wang, *Chem. Sci.*, 2018, **9**, 7986–7991.
60 D. Shao, S.-L. Zhang, L. Shi, Y.-Q. Zhang and X.-Y. Wang, *Inorg. Chem.*, 2016, **55**, 10859–10869.
61 A. Choudhury, P. P. Mudoi, N. Ahmed, D. Deka, S. Sarkar, B. Sarma and N. Gogoi, *Cryst. Growth Des.*, 2023, **23**, 4760–4770.
62 Y. Qin, Y. Wu, S. Luo, J. Xi, Y. Guo, Y. Ding, J. Zhang and X. Liu, *Dalton Trans.*, 2022, **51**, 17089–17096.
63 P. K. Sahu, A. Mondal and S. Konar, *Dalton Trans.*, 2021, **50**, 3825–3831.
64 A. Mondal, S.-Q. Wu, O. Sato and S. Konar, *Chem. – Eur. J.*, 2020, **26**, 4780–4789.
65 L. Chen, J. Wang, J.-M. Wei, W. Wernsdorfer, X.-T. Chen, Y.-Q. Zhang, Y. Song and Z.-L. Xue, *J. Am. Chem. Soc.*, 2014, **136**, 12213–12216.
66 A. E. Thorarinsdottir and T. D. Harris, *Chem. Rev.*, 2020, **120**, 8716–8789.
67 G. M. Espallargas and E. Coronado, *Chem. Soc. Rev.*, 2018, **47**, 533–557.
68 K. Liu, X. Zhang, X. Meng, W. Shi, P. Cheng and A. K. Powell, *Chem. Soc. Rev.*, 2016, **45**, 2423–2439.
69 H. Furukawa, K. E. Cordova, M. O'Keeffe and O. M. Yaghi, *Science*, 2013, **341**, 1230444.
70 X. Zhang, V. Vieru, X. Feng, J.-L. Liu, Z. Zhang, B. Na, W. Shi, B.-W. Wang, A. K. Powell, L. F. Chibotaru, S. Gao, P. Cheng and J. R. Long, *Angew. Chem., Int. Ed.*, 2015, **54**, 9861–9865.
71 Y.-Y. Zhu, M.-S. Zhu, T.-T. Yin, Y.-S. Meng, Z.-Q. Wu, Y.-Q. Zhang and S. Gao, *Inorg. Chem.*, 2015, **54**, 3716–3718.
72 D. Shao, L. Shi, S.-L. Zhang, X.-H. Zhao, D.-Q. Wu, X.-Q. Wei and X.-Y. Wang, *CrystEngComm*, 2016, **18**, 4150–4157.
73 D. Shao, L. Shi, F.-X. Shen and X.-Y. Wang, *CrystEngComm*, 2017, **19**, 5707–5711.
74 D. Shao, L. Shi, H.-Y. Wei and X.-Y. Wang, *Inorganics*, 2017, **5**, 90.
75 M. Roy, A. Adhikary, A. K. Mondal and R. Mondal, *ACS Omega*, 2018, **3**, 15315–15324.
76 X. Liu, X. Ma, P. Cen, F. An, Z. Wang, W. Song and Y.-Q. Zhang, *New J. Chem.*, 2018, **42**, 9612–9619.
77 Z. Chen, L. Yin, X. Mi, S. Wang, F. Cao, Z. Wang, Y. Li, J. Lua and J. Dou, *Inorg. Chem. Front.*, 2018, **5**, 2314–2320.
78 J.-J. Kong, D. Shao, C.-L. Ji, Y.-X. Jiang and X.-C. Huang, *CrystEngComm*, 2019, **21**, 749–757.
79 A. K. Mondal, A. Mondal and S. Konar, *Magnetochemistry*, 2020, **6**, 45.
80 Z. Tian, S. Moorthy, H. Xiang, P. Peng, M. You, Q. Zhang, S.-Y. Yang, Y.-L. Zhang, D.-Q. Wu, S. K. Singh and D. Shao, *CrystEngComm*, 2022, **24**, 3928–3937.
81 D. Shao, S. Moorthy, P. Peng, L. Shi, W.-J. Tang, X.-Q. Wei, Z.-J. Wang and S. K. Singh, *Eur. J. Inorg. Chem.*, 2022, **2022**, e202200354.
82 T. Long, J. Yang, S. Moorthy, D. Shao, S. K. Singh and Y.-Z. Zhang, *Cryst. Growth Des.*, 2023, **23**, 2980–2987.
83 A. K. Seguin, C. Cruz, K. Villafuerte, D. Páez-Hernández, D. Venegas-Yazigi and V. Paredes-García, *Cryst. Growth Des.*, 2023, **23**, 77–86.
84 A. E. Ion, S. Nica, A. M. Madalan, S. Shova, J. Vallejo, M. Julve, F. Lloret and M. Andruh, *Inorg. Chem.*, 2015, **54**, 16–18.
85 X. Liu, L. Sun, H. Zhou, P. Cen, X. Jin, G. Xie, S. Chen and Q. Hu, *Inorg. Chem.*, 2015, **54**, 8884–8886.
86 J. Palion-Gazda, T. Klemens, B. Machura, J. Vallejo, F. Lloret and M. Julve, *Dalton Trans.*, 2015, **44**, 2989–2992.
87 Y.-L. Wang, L. Chen, C.-M. Liu, Y.-Q. Zhang, S.-G. Yin and Q.-Y. Liu, *Inorg. Chem.*, 2015, **54**, 11362–11368.
88 A. K. Mondal, S. Khatua, K. Tomar and S. Konar, *Eur. J. Inorg. Chem.*, 2016, 3545–3552.

89 L. Sun, S. Zhang, S. Chen, B. Yin, Y. Sun, Z. Wang, Z. Ouyang, J. Ren, W. Wang, Q. Wei, G. Xie and S. Gao, *J. Mater. Chem. C*, 2016, **4**, 7798–7808.
90 A. Świtlicka-Olszewska, J. Palion-Gazda, T. Klemens, B. Machura, J. Vallejo, J. Cano, F. Lloret and M. Julve, *Dalton Trans.*, 2016, **45**, 10181–10193.
91 J. Vallejo, F. R. Fortea-Perez, E. Pardo, S. Benmansour, I. Castro, J. Krzystek, D. Armentanoc and J. Cano, *Chem. Sci.*, 2016, **7**, 2286–2293.
92 Y.-L. Wang, L. Chen, C.-M. Liu, Z.-Y. Du, L.-L. Chen and Q.-Y. Liu, *Dalton Trans.*, 2016, **45**, 7768–7775.
93 R. Ma, Z. Chen, F. Cao, S. Wang, X. Huang, Y. Li, J. Lu, D. Lia and J. Dou, *Dalton Trans.*, 2017, **46**, 2137–2145.
94 A. Rodríguez-Diéguez, S. Pérez-Yáñez, L. Ruiz-Rubio, J. M. Seco and J. Cepeda, *CrystEngComm*, 2017, **19**, 2229–2242.
95 D. Shao, L. Shi, H.-Y. Wei and X.-Y. Wang, *Inorganics*, 2017, **5**, 90.
96 D. Shao, Y. Zhou, Q. Pi, F.-X. Shen, S.-R. Yang, S.-L. Zhang and X.-Y. Wang, *Dalton Trans.*, 2017, **46**, 9088–9096.
97 L. Shi, D. Shao, H.-Y. Wei and X.-Y. Wang, *Cryst. Growth Des.*, 2018, **18**, 5270–5278.
98 D. Ma, G. Peng, Y.-Y. Zhang and B. Li, *Dalton Trans.*, 2019, **48**, 15529–15536.
99 L. Shi, F.-X. Shen, D. Shao, Y.-Q. Zhang and X.-Y. Wang, *CrystEngComm*, 2019, **21**, 3176–318540.
100 M. A. Palacios, I. F. Díaz-Ortega, H. Nojiri, E. A. Suturina, M. Ozerov, J. Krzystek and E. Colacio, *Inorg. Chem. Front.*, 2020, **7**, 4611–4630.
101 Y.-R. Qiu, B. Li, Y. Zhou, J. Su and J.-Y. Ge, *CrystEngComm*, 2020, **22**, 3155–3163.
102 A. K. Kharwar, A. Mondal and S. Konar, *Dalton Trans.*, 2021, **50**, 2832–2840.
103 X.-Q. Wei, D. Shao, C.-L. Xue, X.-Y. Qu, J. Chai, J.-Q. Li, Y.-E. Du and Y.-Q. Chen, *CrystEngComm*, 2020, **22**, 5275–5279.
104 D. Shao, S. Moorthy, X. Yang, J. Yang, L. Shi, S. K. Singh and Z. Tian, *Dalton Trans.*, 2022, **51**, 695–704.
105 L.-H. Li, Y. Peng, S. Zhang, T. Xiao, Y. Song, H.-Y. Ye, J. Zhang, Y.-Q. Zhang, Z. Wang and Z.-B. Hu, *Cryst. Growth Des.*, 2023, **23**, 2099–2105.
106 W.-J. Tang, S.-T. Wu, X.-M. Bu, H.-Y. Zhang, X.-Q. Wei and D. Shao, *Polyhedron*, 2023, **229**, 116175.
107 Y. Zhou, S. Moorthy, X.-Q. Wei, S. K. Singh, Z. Tian and D. Shao, *Dalton Trans.*, 2023, **52**, 909–918.
108 Y.-L. Wang, L. Chen, C.-M. Liu, Z.-Y. Du, L.-L. Chen and Q.-Y. Liu, *Dalton Trans.*, 2016, **45**, 7768–7775.
109 G. Brunet, D. A. Safin, J. Jover, E. Ruiz and M. Murugesu, *J. Mater. Chem. C*, 2017, **5**, 835–841.
110 D. Ma, G. Peng, Y.-Y. Zhang and B. Li, *Dalton Trans.*, 2019, **48**, 15529–15536.
111 C. Rajnák and R. Boca, *Coord. Chem. Rev.*, 2021, **436**, 213808.
112 C. E. Jackson, I. P. Moseley, R. Martinez, S. Sung and J. M. Zadrozny, *Chem. Soc. Rev.*, 2021, **50**, 6684–6699.
113 R. Sesooli, *Nature*, 2017, **548**, 400.
114 M. Xu, T. Liang, M. Shi and H. Chen, *Chem. Rev.*, 2013, **113**, 3766–3798.
115 H. Zhang, *Chem. Rev.*, 2018, **118**, 6089–6090.
116 G. Chakraborty, I.-H. Park, R. Medishetty and J. J. Vittal, *Chem. Rev.*, 2021, **121**, 3751–3891.
117 J. Zhang, W. Kosaka, Y. Kitagawa and H. Miyasaka, *Nat. Chem.*, 2021, **13**, 191–199.
118 R. Turo-Cortes, M. C. Munoz, C. Bartual-Murgui, J. Castells-Gil, C. Martı-Gastaldo and J. A. Real, *Chem. Sci.*, 2020, **11**, 11224–11234.
119 S. Chorazy, J. J. Zakrzewski, M. Magott, T. Korzeniak, B. Nowicka, D. Pinkowicz, R. Podgajny and B. Sieklucka, *Chem. Soc. Rev.*, 2020, **49**, 5945–6001.
120 D. Shao, X.-H. Zhao, S.-L. Zhang, D.-Q. Wu, X.-Q. Wei and X.-Y. Wang, *Inorg. Chem. Front.*, 2015, **2**, 846–853.
121 D.-Q. Wu, D. Shao, X.-Q. Wei, F.-X. Shen, L. Shi, D. Kempe, Y.-Z. Zhang, K. R. Dunbar and X.-Y. Wang, *J. Am. Chem. Soc.*, 2017, **139**, 11714–11717.
122 S.-L. Zhang, X.-H. Zhao, Y.-M. Wang, D. Shao and X.-Y. Wang, *Dalton Trans.*, 2015, **44**, 9682–9690.
123 X.-Q. Wei, Q. Pi, F.-X. Shen, D. Shao, H.-Y. Wei and X.-Y. Wang, *Dalton Trans.*, 2018, **47**, 11873–11881.
124 X.-H. Zhao, D. Shao, J.-T. Chen, D.-X. Gan, J. Yang and Y.-Z. Zhang, *Sci. China: Chem.*, 2022, **65**, 532–538.
125 J. Wang, J. J. Zakrzewski, M. Zychowicz, Y. Xin, H. Tokoro, S. Chorazy and S. Ohkoshi, *Angew. Chem., Int. Ed.*, 2023, **62**, e202306372.
126 P. Tin, A. N. Bone, N. N. Bui, Y.-Q. Zhang, T. Chang, D. H. Moseley, M. Ozerov, J. Krzystek, Y. Cheng, L. L. Daemen, X. Wang, L. Song, Y.-S. Chen, D. Shao, X.-Y. Wang, X.-T. Chen and Zi-Ling Xue, *J. Phys. Chem. C*, 2022, **126**(31), 13268–13283.
127 J.-P. Zhang, X.-C. Huang and X.-M. Chen, *Chem. Soc. Rev.*, 2009, **38**, 2385–2396.
128 Y.-S. Meng, S.-D. Jiang, B.-W. Wang and S. Gao, *Acc. Chem. Res.*, 2016, **49**, 2381–2389.
129 C. E. Jackson, I. P. Moseley, R. Martinez, S. Sung and J. M. Zadrozny, *Chem. Soc. Rev.*, 2021, **50**, 6684–6699.
130 S. K. Gupta, S. V. Rao, S. Demeshko, S. Dechert, E. Bill, M. Atanasov, F. Neese and F. Meyer, *Chem. Sci.*, 2023, **14**, 6355–6374.
131 X.-R. Wu, S.-Q. Wu, Z.-K. Liu, M.-X. Chen, J. Tao, O. Sato and H.-Z. Kou, *Nat. Commun.*, 2024, **15**, 3961.
132 Y.-X. Wang, Y. Ma, Y. Chai, W. Shi, Y. Sun and P. Cheng, *J. Am. Chem. Soc.*, 2018, **140**, 7795–7798.
133 Y.-X. Wang, D. Su, Y. Ma, Y. Sun and P. Cheng, *Nat. Commun.*, 2023, **14**, 7901.
134 M. Darawsheh, L. A. Barrios, O. Roubeau, S. J. Teat and G. Aromí, *Angew. Chem., Int. Ed.*, 2018, **57**, 13509–13513.
135 O. Sato, *Nat. Chem.*, 2014, **8**, 644–656.
136 X.-D. Huang, X.-F. Ma and L.-M. Zheng, *Angew. Chem., Int. Ed.*, 2023, **62**, e202300088.
137 Y. Xin, J. Wang, M. Zychowicz, J. J. Zakrzewski, K. Nakabayashi, B. Sieklucka, S. Chorazy and S. Ohkoshi, *J. Am. Chem. Soc.*, 2019, **141**, 18211–18220.
138 J. J. Zakrzewski, M. Liberka, J. Wang, S. Chorazy and S. Ohkoshi, *Chem. Rev.*, 2024, **124**, 5930–6050.

